A Quantized Classical Path Approach for Calculations of Quantum Mechanical Rate Constants

Jenn-Kang Hwang† and Arieh Warshel*

Department of Chemistry, University of Southern California, Los Angeles, California 90089-1062

Received: May 27, 1993®

A practical method for calculations of quantized rate constants is examined and illustrated. The method, which is referred to as the "quantized classical path" approach, evaluates quantum mechanical activation energies by propagating trajectories of the classical particles to generate the centroid positions for the quantum mechanical calculations. This provides a stable and effective way for evaluating quantized activation energies of processes in multidimensional systems. In fact, the present approach was used before in studies of proton-transfer and hydride-transfer reactions in solution and proteins (Hwang et al. *J. Phys. Chem.* **1991**, *95*, 8445), but its validity was not established in well-defined test cases. The present work compares the results of the quantized classical path method to that of a quantum mechanical calculation of the reactive flux for an Eckart potential coupled to harmonic oscillators (McRae et al. *J. Chem. Phys.* **1992**, *97*, 7392) and demonstrates that our approach provides reliable results. We also illustrate the performance of our method in evaluation of partition functions by considering the HCl system studied recently (Topper et al. *J. Chem. Phys.* **1992**, *97*, 3668), demonstrating accuracy and fast convergence. Finally, the applicability of the method to multidimensional problems is illustrated by calculating isotope effects in a proton-transfer reaction in aqueous solution.

Introduction

The search for an effective prescription for evaluation of quantum mechanical rate constants has recently become the subject of significant interest.[1-5] Substantial progress has been made in the development of methods to evaluate quantum mechanical rate constants of reactions in solutions.[5-10] The use of microscopic simulations in evaluating quantum mechanical rate constants for diabatic reactions has progressed significantly in recent years, and several approaches with reasonable convergence have been developed.[5a,6a,7,8] On the other hand, the development of practical methods to calculate rate constants of adiabatic reactions has been slower. Several path integral methods have been introduced and examined on systems with few degrees of freedom, but the application of such methods to reactions in solutions has been quite limited.[5a,5b,9a] Furthermore, convergence problems are expected from some of the proposed methods (when the quantum simulations are extended to the complete dimensionality of the system).

Our effort in this field has been focused on the evaluation of quantum mechanical rate constants for charge-transfer reactions in solutions and proteins.[5,7] To reduce the convergence problem, we developed an approach that utilizes trajectories of the classical particles to obtain the centroid positions for the quantum mechanical calculations. This approach is referred to here as *the quantized classical path* (QCP) method. While the simplicity and effectiveness of our approach has been demonstrated, it was not established using well-defined test cases. This work examines the reliability of the QCP method by using it in studies of simple test cases. The results of this examination are very encouraging considering the simple and direct implementation of this method in studies of chemical reactions in solution and proteins.

The QCP Method

The quantum mechanical rate constants can be expressed as

$$k = \kappa \frac{k_B T Z^{\ddagger}}{h\ Z_R} = \kappa \frac{k_B T}{h} \exp(-\beta \Delta g^{\ddagger}) \qquad (1)$$

where κ is the transmission factor, k_B the Boltzmann constant, T temperature, and h the Plank constant. $Z^{\ddagger}$ and Z_R are the partition functions at the transition state and reactant state, respectively. β is $1/k_B T$, and $\Delta g^{\ddagger}$ is the activation free energy. The largest quantum effects are associated with the partition function, which is the primary subject of our approach. The QCP strategy for evaluating Z has been given elsewhere.[5b] Here we will provide an alternative derivation. Our starting point is the Feynman's path integral representation of the quantum mechanical partition function[11,12]

$$Z = \int \mathrm{D}x(\tau) \exp\left\{-\frac{1}{h}\int_0^{\beta h} \mathrm{d}\tau \left[\frac{m x(\tau)^2}{2} + V(x(\tau))\right]\right\} \qquad (2)$$

The path $x(\tau)$ can be decomposed into the Fourier components

$$x(\tau) = x_0 + \sum_{n=1}^{\infty} x_n \exp(-i\Omega_n \tau) + x_{-n} \exp(i\Omega_n \tau) \qquad (3)$$

where $\Omega_n = 2n\pi/\beta h$ and the zero Fourier component x_0 is given by

$$x_0 = \frac{1}{\beta h}\int_0^{\beta h} \mathrm{d}\tau\, x(\tau) \qquad (4)$$

In the Fourier path integral (FPI) representation the quantum mechanical partition function is

$$Z = \int \mathrm{d}x_0\, \rho(x_0) = \int \frac{\mathrm{d}x_0}{(2\pi h^2 \beta/m)^{1/2}} \int \prod_{n=1}^{\infty} \frac{\mathrm{d}\,\mathrm{Re}\, x_n\, \mathrm{d}\,\mathrm{Im}\, x_n}{\pi/\beta\Omega_n{}^2 m} \times \exp\left(-\beta \sum_{n=1}^{\infty} m\Omega_n{}^2 |x_n|^2 + \frac{1}{h\beta}\int_0^{h\beta} V[x(\tau)]\, \mathrm{d}\tau\right) \qquad (5)$$

Multiplying eq 5 by $\exp(-\beta V(x_0))\ \exp(\beta V(x_0))$, we obtain

$$Z = \int \frac{\mathrm{d}x_0}{(2\pi h^2 \beta/m)^{1/2}} \int \prod_{n=1}^{\infty} \frac{\mathrm{d}\,\mathrm{Re}\, x_n\, \mathrm{d}\,\mathrm{Im}\, x_n}{\pi/\beta\Omega_n{}^2 m} \exp[-\beta(V(x_0) + \sum_{n=1}^{\infty} m\Omega_n{}^2 |x_n|^2)] \exp\left\{\frac{1}{h}\int_0^{h\beta} [V[x(\tau)] - V(x_0)]\, \mathrm{d}\tau\right\} \qquad (6)$$

† Present address: Institute of Life Sciences, National Tsing Hua University, Hsin Chu, Taiwan.

• Abstract published in *Advance ACS Abstracts*, September 1, 1993.

0022-3654/93/2097-10053$04.00/0

If we define an effective potential $V_{eff}(x)$

$$V_{eff}(x) = V(x_0) + \sum_{n=1}^{\infty} m\Omega_n^2|x_n|^2 \tag{7}$$

and use the following identity

$$\int \prod_{n=1}^{\infty} \frac{d\,\mathrm{Re}\,x_n\, d\,\mathrm{Im}\,x_n}{\pi/\beta\Omega_n^2 m} \exp(-\beta \sum_{n=1}^{\infty} m\Omega_n^2|x_n|^2) = 1$$

then eq 6 can be recast in the following form

$$Z = Z_{cl}\langle \exp[-\beta(\bar{V} - V)]\rangle_{eff} \tag{8}$$

where Z_{cl} is the classical partition function and $\bar{V}$ is given by

$$\bar{V} \equiv \frac{1}{\beta h}\int_0^{\beta h} V[x(\tau)]\, d\tau \tag{9}$$

and

$$\langle(...)\rangle_{eff} = \frac{\int dx_0 \prod_{n=1}^{\infty} d\,\mathrm{Re}\,x_n\, d\,\mathrm{Im}\,x_n \exp(-\beta V_{eff}(x))(...)}{\int dx_0 \prod_{n=1}^{\infty} d\,\mathrm{Re}\,x_n\, d\,\mathrm{Im}\,x_n \exp(-\beta V_{eff}(x))} \tag{10}$$

Thus the quantum correction of the partition function can be obtained by calculating the ensemble average of $\langle \exp[-\beta(\bar{V} - V)]\rangle_{eff}$ over the effective potential $V_{eff}(x)$. The interesting point about the effective potential is that the motion of the system can be separated into that of the center of mass (COM), which is defined by $x_0(t)$, and that of the rest of the quasiparticles. The trajectory of the COM moves only on the potential $V(x)$, while the rest of the quasiparticles perform harmonic oscillation relative to the COM. These two kinds of trajectories can be solved independently. That is, we can rewrite eq 8 as

$$Z = Z_{cl}\langle \langle \exp\{-\beta(\bar{V} - V)\}\rangle_{fp}\rangle_{v} \tag{11}$$

where $\langle ... \rangle_v$ corresponds to an average over the distribution function of $V(x_0)$ and in the case of multidimensional systems it is obtained by propagating classical trajectories over V. Here $\langle ... \rangle_{fp}$ designates an average over the free particle distribution function

$$\langle(...)\rangle_{fp} = \frac{\int \prod_{n=1}^{\infty} d\,\mathrm{Re}\,x_n\, d\,\mathrm{Im}\,x_n \exp(-\beta \sum_{n=1}^{\infty} m\Omega_n^2|x_n|^2)(...)}{\int \prod_{n=1}^{\infty} d\,\mathrm{Re}\,x_n\, d\,\mathrm{Im}\,x_n \exp(-\beta \sum_{n=1}^{\infty} m\Omega_n^2|x_n|^2)} \tag{12}$$

Thus we can calculate the quantum mechanical partition function for multidimensional systems by simply propagating the classical trajectories of the COM over the potential $V(x)$ and calculating the quantum correction $\langle \exp[-\beta(\bar{V} - V)]\rangle_{fp}$ along the way. This average is obtained by the descretized path integral (DPI) approach where each classical particle is represented by P quasiparticles $(x_1, x_2, ..., x_p)$ propagated by either Monte Carlo or Langevin dynamics on the effective potential[5b] which requires that $\sum_i x_i/P = x_0$. The two types of trajectories needed for the evaluation of eq 11 can be propagated with different time steps and different procedures, as illustrated in Figure 1.

It should be noted that the primary result of our approach is not the derivation of eq 11 but the idea that one can use classical trajectories for the average over x_0 and then obtain the quantum free energy by performing a fp average. In fact, eq 8, which is similar to a related expression of Doll and Myers,[14a] is merely presented here as an alternative to the derivation of eq 11 by the method of ref 5b. The rigorous derivations are important, since the simple form of eq 11 has led some to believe that this is an approximate expression such as that used with the effective potential of Feynman and Hibbs,[12a] despite the fact that eqs 8 and 11 are formally exact. We would also like to emphasize that the *use* of a double average in centroid calculations is new and this new idea is the main point of the QCP method.

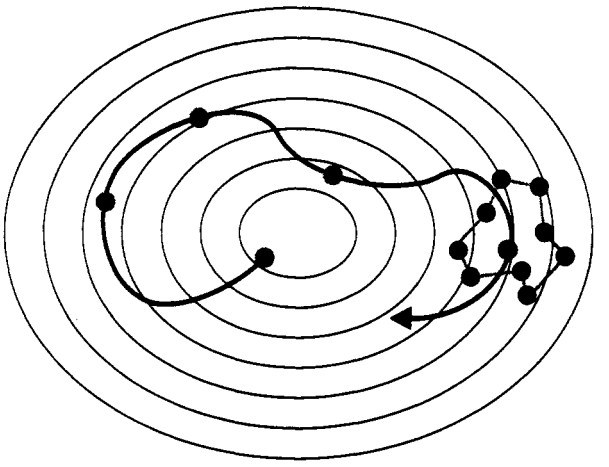

Figure 1. Schematic illustration of the implementation of the QCP method. The figure depicts a classical trajectory over the given potential and a polymer of P quasiparticles which is centered around the coordinates of the classical path. More specifically, the classical trajectory is used to generate the path $x(\tau)$, and the quantum mechanical partition function is then evaluated by using Langevin dynamics to propagate P quasiparticles over the free-particle effective potential while requiring that $\sum_i x_i/P = x$.

Frequently it is more convenient to run the trajectory on a mapping potential V_m than on the given potential V. In this case Z is written as

$$Z = Z_{cl}^{m}\langle \exp\{-\beta[\bar{V} - V_m]\}\rangle_{eff} \tag{13}$$

where Z_{cl}^{m} is the classical partition function for V_m and the effective potential has the same form as before except with V replaced by V_m. This equation is especially useful in the free energy perturbation (FEP) calculations where V is taken as V_m and Z_{cl} as Z_{cl}^{m}.

Our main interest in the present work is in rate constants and activation free energies, rather than in ground-state partition functions. Thus we would like to use the QCP method to evaluate the Z^* of eq 1. This is done by evaluating the probability function $\rho(x)$ of eq 5 along the reaction coordinate of our system, x. With the present formulation we can write (see also derivation in ref 5b)

$$\rho(x) = Z_{cl}[\int dx_0 \prod_{n=1}^{\infty} d\,\mathrm{Re}\,x_n\, d\,\mathrm{Im}\,x_n \times \exp(-\beta V_{eff}(x))\delta(x-x_0) \exp[-\beta(\bar{V} - V(x_0))]/ \int dx_0 \prod_{n=1}^{\infty} d\,\mathrm{Re}\,x_n\, d\,\mathrm{Im}\,x_n \exp(-\beta V_{eff}(x))] = Z_{cl}\langle \delta(x-x_0) \exp\{-[\beta(\bar{V} - V(x_0))]\}\rangle_{eff} \tag{14}$$

A direct evaluation of eq 14 might be impractical for transition states whose energies are much larger than $1/\beta$. In such cases it is important to use FEP/umbrella sampling methods of the form described in ref 5. In this case we can write the corresponding expression as

$$\rho(x) = Z_{cl}^{m}\langle \delta(x-x_0) \exp\{-[\beta(\bar{V} - V_m(x_0))]\}\rangle_{eff} = Z_{cl}^{m}\langle \delta(x-x_0)\langle \exp\{-[\beta(\bar{V} - V_m(x_0))]\}\rangle_{fp}\rangle_{V_m} \tag{15}$$

and finally $Z^* = (2\pi h^2\beta/m\rho(x^*))^{1/2}$ can be used to evaluate eq 1.

TABLE I: Comparison of QCP Results of Vibrational-Rotational Partition Functions with Corresponding Results of the Exact Calculations

T	Z_{calc}	Z_{qu}[a]
300	0.0161	0.01651
400	0.1240	0.1300
500	0.4726	0.4718
600	1.11	1.153
900	5.40	5.713
1200	13.47	14.11
2000	51.7	53.55
4000	250	257.5
5000	409	421.0
6000	629	630.5

[a] Reference 17.

It is instructive to note[5a] the difference between $\rho(x)$ and the density matrix element $\rho'(x,x)$ derived in ref 14b. $\rho(x,x)$ values express the probability of moving from x to x, while the $\rho(x)$ gives the quantum mechanical probability of being at x. Apparently $\rho'(x,x)$ can only be used in direct evaluation of activation barriers (e.g. by using the flux–flux autocorrelation[14b]) or in providing semiclassical estimates of $\Delta g^{\ddagger}$ (see discussion in ref 5b). Nevertheless, obtaining the $\Delta g^{\ddagger}$ of eq 1 from the $\rho(x)$ defined by eq 14 is not based on a fundamental derivation but on a reasonable assumption.

The present treatment and that of ref 5b are related to the centroid formulation of Gillan[2] and Voth et al.,[3] but the use of classical trajectories as the basis for the evaluation of the quantized ρ is new. More specifically, centroid simulations evaluate trajectories under the effective potential $\sum_{n=1}^{P}(m\Omega^2/2P)(x_{n-1} - x_n)^2 + V_m/P$ (where we consider for simplicity the one-dimensional case). The relevant contribution to the quantum activation energy is collected whenever the centroid of the P quasiparticles coincides with a specific x_0. On the other hand, the QCP method evaluates the trajectory of the classical particle (or particles) under the potential V_m and then obtains the quantum average of eq 15 by integrating the motion of the quasiparticles, considering only the effect of the free particle potential $\sum_{n=1}^{P}(m\Omega^2/2P)(x_{n-1} - x_n)^2$. This treatment does not require evaluation of forces $\delta V_m/\delta x_k$ during quantum calculations. Furthermore, the fp average can be performed in larger time intervals than that needed for the calculation of the classical trajectory.

Results and Discussion

1. Calculations of Partition Functions. In order to examine the performance of the QCP method in evaluation of quantum mechanical partition functions, we considered the test case of the HCl molecule. The vibrational–rotational Hamiltonian of the system[17] is given by

$$\mathcal{H} = -\frac{h^2}{2\mu}\sum_{i=1}^{3}\frac{\partial^2}{\partial x_j^2} + D_e[(1 - e^{-y})^2 + cy^3e^{-y}(1 + by)] \qquad (16)$$

where

$$y = \frac{\omega_e}{2(B_eD_e)^{1/2}}\left(\frac{r - r_e}{r_e}\right) \qquad (17)$$

$$r = (x^2 + y^2 + z^2)^{1/2}$$

The actual parameters of this Hamiltonian are given in ref 17. The partition function of this system was evaluated by the QCP approach. The trajectory of the center of mass is propagated in the Cartesian space using Langevin dynamics, and the quasiparticles are treated using the descritized path integral formulation. The result is given in Table I. The agreement between quantum mechanical calculations[17] and the QCP results is quite satisfactory, considering the fact that the maximal P used in our calculations is only 60 compared to 1024 in ref 17.

2. Rate Constants for Eckart Potential Coupled to Harmonic Oscillators. Next we examined the performance of the QCP method in calculations of rate constants for the test case[4] that involves a one-dimensional solute, linearly coupled to N harmonic oscillators

$$\mathcal{H} = \frac{p_q^2}{2\mu} + V(q) + \sum_{j=1}^{N}\frac{P_j^2}{2\mu} + \frac{\mu\omega_j^2}{2}(Q_j - c_jq)^2 \qquad (18)$$

where q and Q_j are the solute and solvent coordinates, p_q and P_j are their conjugated momenta, μ is the reduced mass, ω_j is the solvent harmonic frequency, and c_j is the coupling constant. The classical motion of this system can be described by the general Langevin equation (GLE)

$$\mu\ddot{q} = -\frac{dV}{dt} - \int_0^t dt'\,\eta(t-t')(p_q/\mu) + F(t) \qquad (19)$$

where $\eta(t)$ is the friction kernel

$$\eta(t) = \sum_{j=1}\mu c_j^2\omega_j^2\cos\omega_j t \qquad (20)$$

and $F(t)$ the random force. The solute potential $V(q)$ is given by the symmetric Eckart potential

$$V(q) = V_0\,\mathrm{sech}^2\frac{\alpha q}{2} \qquad (21)$$

where the parameters $\alpha = 3.97$ Å and $V_0 = 9.80$ kcal/mol are chosen to mimic the H + H_2 gas-phase reaction. The reduced mass μ is 0.672 amu. For later use, we introduce the harmonic frequency of the barrier top, $\omega_b = (\alpha^2V_0/2\mu)^{1/2}$. In the case of Gaussian friction kernel, i.e.

$$\eta(t) = \frac{\eta_0}{\sigma}\left(\frac{2}{\pi}\right)^{1/2}\exp(-t^2/2\sigma^2)$$

the coupling constant can be shown to be[4]

$$c_j^2 = \frac{2f|\omega_b|}{\tau\omega_j^2}\exp(-\omega_j^2\sigma^2/2) \qquad (22)$$

where f is the reduced friction

$$f = \frac{\eta_0}{\mu\omega_b} \qquad (23)$$

The bath parameters used in the calculations are given in Table II. For simplicity, we calculate the case with $N = 1$, though it should be noted that QCP can very easily be applied to a multidimensional system.

Different studies have demonstrated that the pre-exponential factor of eq 1 is similar in the classical and quantum mechanical cases. However it is useful to have an estimate of the quantum effect on the factor. This is done by starting with the classical transmission factor[15]

$$\kappa = \frac{\lambda}{\omega_b} \qquad (24)$$

where ω_b is the "bare" frequency at the barrier top and λ is the effective reactive frequency which satisfies the following equation

$$\lambda = \frac{\omega_b^2}{\lambda + \tilde{\eta}(\lambda)/\mu} \qquad (25)$$

where $\tilde{\eta}$ is the Laplace transform of the friction kernel $\eta(t)$.

In order to obtain the corresponding quantum mechanical transmission factor, we will replace ω_b by the effective frequency Ω_b, which is calculated by the following iterative equations[11,16,18]

$$\Omega_b^2 = -\frac{1}{\mu}\frac{\partial^2}{\partial x^2}V_a(x) \qquad (26a)$$

TABLE II: Comparing the Reactive Flux Obtained by the QCP Approach to That Obtained by Quantum Mechanical Calculations[a]

f[b]	QM[c]	QCP
	Slow Friction	
0	15260	12070
4	3100	2769
8	1036	956.9
15	92.44	179.1
20	27.56	37.4
30	6.496	7.02
40	2.352	2.46
60	0.5165	0.541
	Medium Friction	
0	2968	2263
1	518.2	469.7
2	74.38	156.9
5	11.56	14.17
10	1.068	1.34
20	6.839E-2	8.283E-2
40	1.886E-3	2.523E-3
	Fast Friction	
0	90.46	65.25
1	3.749	3.69
2	0.581	0.570
10	3.432E-4	3.750E-4
20	1.686E-6	2.215E-6

[a] The calculations are performed for different ranges of the reduced friction, f, at 200 K. The parameters for different baths are given respectively by, (i) for slow-friction bath, σ = 86.6 fs, τ/σ = 2, and ω_1 = 48 cm^{-1}; (ii) for medium-friction bath, σ = 18.48 fs, τ/σ = 2, and ω_1 = 226 cm^{-1}; and (iii) for fast-friction bath, σ = 3.696 fs, τ/σ = 2, and ω_1 = 1128 cm^{-1}. [b] The reactive flux J is defined by $J = Z_R k$. [c] Reference 4.

$$a^2 = \frac{2}{\beta\mu}\sum \frac{1}{\omega_n^2 + \Omega_b^2 + \omega_n\tilde{\eta}(\omega_n)/\mu} \qquad (26b)$$

where $\omega_n = 2n\pi/h\beta$ and the smeared function $V_a(x)$ is given by

$$V_a(x) = \int \frac{dy}{(2\pi a^2)^{1/2}} \exp(-(x-y)^2/2a^2)V(y) \qquad (27)$$

The quantum mechanical version of the transmission factor is simply given by[16]

$$\kappa = \frac{\lambda}{\Omega_b} \qquad (28)$$

The calculations of the quantum paths for the fp average were done using a Brownian dynamics simulation technique[2,5b,13] (see ref 13 for details). The constrained quantum path is integrated using a potential that only reflects the temperature-dependent harmonic forces within the quantum path and is independent of the forces of the system (or the mapping potential). The energy of the quantum path is calculated by projecting it back to the original classical configuration space. Since in our formulation the motions of the classical particles are independent of the constraint quantum paths, these two kinds of trajectories can be integrated separately, thus offering a great advantage in the numerical implementation; the subroutines that calculate the quantum path can be directly plugged into any standard molecular simulation software without significant effort (the path calculations involve only the free particles' potential and do not require any connection to the force calculations in the main program).

It is important to note that our calculation locates the transition state at the surface defined by $Q = 0$, rather than by searching the optimal dividing surface separating the reactant and product states. Apparently, even this crude approximation gives reasonable results, perhaps reflecting the fact that calculations that evaluate the transmission factor should give similar results for different selections of the transition state.

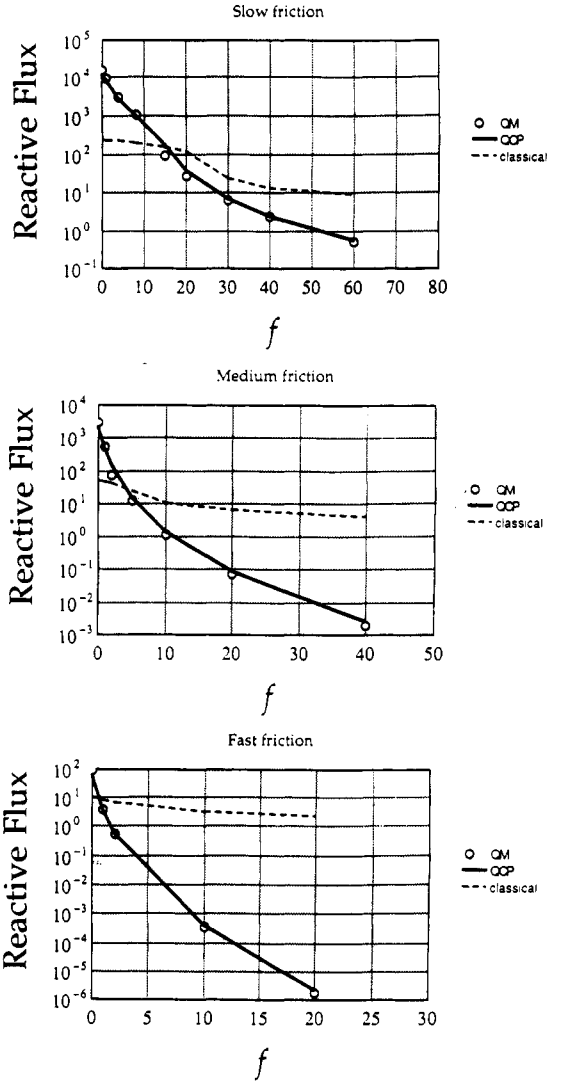

Figure 2. Reactive flux at 200 K as a function of reduced friction, f, for an Eckart potential which is linearly coupled to a single harmonic oscillator. Results for the quantum mechanical (circle), classical (dotted line), and QCP (solid line) calculations are shown for (a) slow, (b) medium, and (c) fast frictions.

Our results are given in Table II. The agreement between the quantum mechanical (QM) and QCP calculations appears to be reasonably good. The QM, QCP, and classical results are plotted as functions of reduced friction in Figure 2 for (a) slow, (b) medium, and (c) fast frictions. It is seen from the figure that the classical results are quite different from the QM ones, but the QCP results (the classical values multiplied by the quantum corrections) are encouraging. Our results are very similar to that obtained for the same system by regular centroid calculations,[4] and in fact the two approaches should give similar results, since they differ only in the way the average is being done. However, in the case of multidimensional systems the QCP strategy is expected to converge faster (see below).

3. Quantized Rate Constants for Proton-Transfer Reactions in Solutions. After demonstrating the performance of the QCP method in well-defined test cases, it is instructive to illustrate the application of this method in a realistic proton-transfer (PT) reaction in solution. Here we consider the reaction

$$AH + B^- \rightarrow A^- + HB \qquad (29)$$

The reacting system is described by the empirical valence bond (EVB) method,[21] considering the two resonance structures

$$\psi_1 = [A\text{–}H\ B^-]\phi_1$$

$$\psi_2 = [A^- H\text{–}B]\phi_2 \quad (30)$$

where the ϕ is the wave function for the solvent and the solute electrons not included in the AHB system. Note that these two resonance structures include the effect of the high-energy state ($A^-H^+B^-$).[21] The potential surface for the two-state valence bond (VB) model is obtained by solving the secular equation

$$\begin{vmatrix} H_{11} - E & H_{12} - S_{12}E \\ H_{21} - S_{21}E & H_{22} - E \end{vmatrix} \quad (31)$$

where the matrix elements of H can be obtained by performing gas-phase *ab initio* calculations or represented by semiempirical analytical potential functions. The diagonal matrix elements are given by

$$H_{11} = H_{11}^{\,0} + V_{Ss}^{\,1} + V_{ss} \quad (32)$$

$$H_{22} = H_{22}^{\,0} + V_{Ss}^{\,2} + V_{ss}$$

where $V_{Ss}^{\,i}$ is the interaction between the ith resonance structure of the solute S (i.e. A, H, and B) and the solvent s and V_{ss} is the solvent–solvent interaction. The overlap integral S_{12} is absorbed into the semiempirical H_{12}, and the solute–solvent interaction is described by analytical functions. The matrix element for the isolated solute is represented by

$$H_{11}^0 = D_e[\exp(-\mu_1(r_{AH} - r_0)) - 1]^2 + \frac{q_B q_H}{r_{BH}} + \frac{q_A q_B}{r_{AB}} + C\exp(-\mu_2 r_{BH}) + C\exp(-\mu_2 r_{AB}) \quad (33)$$

$$H_{22}^0 = D_e[\exp(-\mu_1(r_{BH} - r_0)) - 1]^2 + \frac{q_A q_H}{r_{AN}} + \frac{q_A q_B}{r_{AB}} + C\exp(-\mu_2 r_{AH}) + C\exp(-\mu_2 r_{AB}) + \Delta$$

$$H_{12} = A_{12}\exp[-\mu_3 r_{AB}]$$

The relevant parameters in eq 33 are given by D_e = 110 kcal/mol, r_0 = 1 Å, α_1 = 2.9 Å^{-1}, $q_{A(B)}$ (of A(B)–H) = –0.2, $q_{A(B)}$ (of isolated A(B)) = –1.0 where A(B) designates A or B, q_H = 0.2, C = 50 kcal/mol, μ_2 = 2.5 Å^{-1}, A_{12} = 50 kcal/mol, and μ_3 = 0.4 Å^{-1}. The masses of atoms A and B correspond to that of the oxygen atom, 12 amu. The solvent–solute interactions include the electrostatic and 6–12 Lennard-Jones interactions, and the parameters of A(B) and H are identical to those of 'O1' and 'H1' and 'H1' defined in ENZYMIX.[18] The parameter Δ is treated as an adjustable parameter so that the dependence of the rate constant on the free energy of the reaction can be examined in a systematic way. The water molecules around the reacting atoms were treated by the SCAAS model.[20] The simulation sphere included the solute and 150 solvent molecules within a sphere of radius 10 Å. A cutoff of 8 Å was used for the nonbonded interactions. The A and B atoms were constrained at a distance of 2.6 Å. The simulation was performed at a temperature of 300 K with an integration step size of 1 fs. The mapping potential was represented by the function $V_m(\theta) = \theta V_1 + (1-\theta)V_2$, where θ is the mapping parameter and V_i is the diabatic potential of the ith resonance structure. θ was changed from zero to one in ten mapping steps. The total simulation time was 100 ps (following 20-ps equilibration time), and since our reaction is symmetrical, we averaged the data from the corresponding mapping steps and this procedure in effect doubles our simulation time to 200 ps. Figure 3a and b compares the classical and quantum mechanical free energy profiles for the proton-transfer reaction. We also checked the effect of $\Delta G°$ on the kinetic isotope effect (K.I.E.). Our result is shown in Figure 4, which indicates that the QCP calculation is reliable enough to reproduce the general characteristics of the K.I.E. curve as a function of $\Delta G°$.

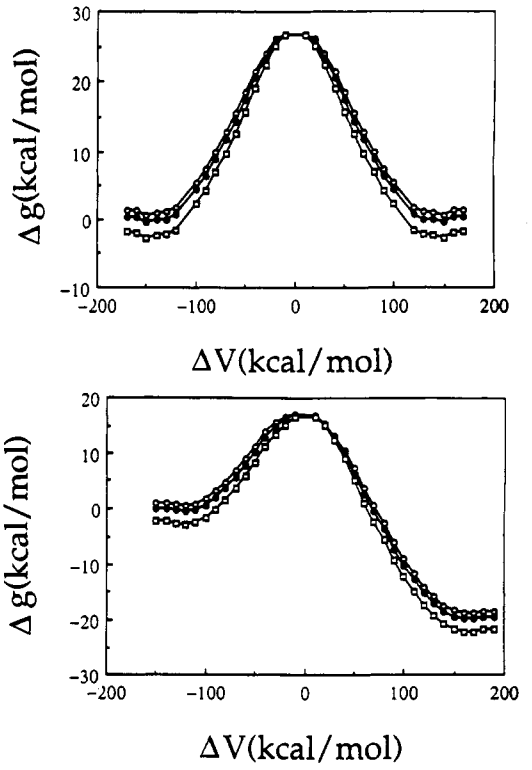

Figure 3. Quantum mechanical and classical free energy profiles for a proton-transfer reaction in aqueous solution (the model system studied is described in the text). The open circles denote the QCP calculations for an H atom, the filled circles for a D atom, while the squares denote the results obtained by the usual classical FEP calculations. Part a is obtained with $\Delta G°$ = 0.0 kcal/mol, while Part b is obtained with $\Delta G°$ = 20 kcal/mol.

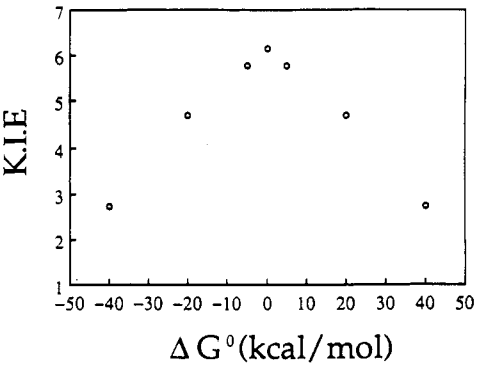

Figure 4. Kinetic isotope effect (K.I.E.) obtained by the QCP calculations. The K.I.E. attains its maximum when $\Delta G°$ is zero and falls off when the absolute value of $\Delta G°$ increases.

Concluding Remarks

Path integral calculations of quantum partition functions and activation free energies present a significant computational challenge. The efficiency of such calculations depends on the ability of the "polymers" of the quasiparticles to explore the relevant phase space. When P is large, the harmonic forces between the quasiparticles become very strong and the evaluation of the trajectories of these particles requires the use of small time steps, thus hindering the polymers from effectively spanning the phase space. The QCP approach reduces this problem by allowing one to rigorously[22] separate the oscillatory motion of the individual quasiparticles from the translational motion of the centers of mass of the polymers. The moves of the centers of mass are identified with the trajectories of the corresponding classical particles, while the motions of the quasiparticles are described by simple harmonic oscillations relative to their centers of mass. The independence of these two motions allows the polymers to effectively explore the phase space and ensures rapid convergence.

This paper did not compare the performances of the QCP to that of the regular centroid calculations. The reason is that, for one-dimensional problems and for cases where the position of the transition state is known, the two approaches are almost equivalent. The real difference appears in multidimensional FEP/umbrella sampling calculations, e.g. (eq 15). In such calculations, the QCP approach involves classical trajectories of only $3N$ particles (for N atom systems) and once in several time steps a fp average over the quasiparticles. On the other hand, the regular centroid sampling involves trajectories of $3NP$ quasiparticles. Thus the QCP simulation is expected to converge faster. Furthermore, the QCP approach does not require the evaluation of the forces associated with the quasiparticles, and it can greatly benefit from using the results of classical FEP calculations (since it evaluates the quantum correction to the classical partition function rather than the quantum partition function). Nevertheless, the actual comparison of the QCP to alternative multidimensional approaches is left for further studies.

One of the most appealing features of the QCP method is its convenient implementation. That is, the method can be incorporated into standard MD simulation programs without significant effort, where the integration over the quantum path is done in a few separated subroutines. In the present study we combined the QCP approach with the EVB method by introducing only minor modifications to the ENZYMIX[19] program. This provides a general way of evaluating quantum mechanical corrections to rate constants of charge-transfer reactions in solutions and proteins.

Acknowledgment. We are grateful to Dr. Schenter for making ref 4 available to us before publication. This work was supported by the office of Naval Research Grant No. N00014-91-5-1318 and by Grant No. GM24492 from the National Institutes of Health.

References and Notes

(1) Truhlar, D. G.; Isaacson, A. D.; Garrett, B. C. In *CRC Theory of Chemical Reaction Dynamics*; Baer, M., Ed.; CRC Press: Boca Raton, FL, 1985; Vol. IV, p 65.

(2) Gillan, M. J. *J. Phys. C* **1987**, *20*, 3621.

(3) Voth, G. A.; Chandler, D.; Miller, W. H. *J. Chem. Phys.* **1989**, *91*, 7749.

(4) McRae, R. P.; Schenter, G. K.; Garrett, B. C.; Haynes, G. R.; Voth, G. A.; Schatz, G. C. *J. Chem. Phys.* **1992**, *97*, 7392.

(5) (a) Warshel, A.; Chu, Z. T. *J. Chem. Phys.* **1990**, *93*, 4003. (b) Hwang, J.-K.; Chu, Z. T.; Yadav, A.; Warshel, A. *J. Phys. Chem.* **1991**, *95*, 8445.

(6) (a) Wolynes, P. G. *J. Chem. Phys.* **1987**, *87*, 6559. (b) Zheng, C.; McCammon, J. A.; Wolynes, P. G. *Chem. Phys.* **1991**, *158*, 261.

(7) Warshel, A.; Hwang, J.-K. *J. Chem. Phys.* **1986**, *84*, 4938.

(8) Bader, J. S.; Kuharski, R. A.; Chandler, D. *J. Chem. Phys.* **1990**, *93*, 203.

(9) (a) Lobaugh, J.; Voth, G. A. *Chem. Phys. Lett.* **1992**, *198*, 311. (b) Li, D.; Voth, G. A. *J. Phys. Chem.* **1991**, *95*, 10425.

(10) (a) Borgis, D.; Lee, S.; Hynes, J. T. *Chem. Phys. Lett.* **1989**, *162*, 19. (b) Borgis, D.; Hynes, J. T. *J. Chem. Phys.* **1991**, *94*, 3619.

(11) Feynman, R. P.; Kleinert, K. *Phys. Rev. A* **1986**, *34*, 5080.

(12) (a) Feynman, R. P.; Hibbs, A. R. *Quantum Mechanics and Path Integrals*; McGraw-Hill: New York, 1965. (b) Feynman, R. P. *Statistical Mechanics*; Benjamin: New York, 1972.

(13) Allen, M. P. *Mol. Phys.* **1980**, *40*, 1073.

(14) (a) Doll, J. D.; Myers, L. E. *J. Chem. Phys.* **1979**, *71*, 2889. (b) Doll, J. D. *J. Chem. Phys.* **1984**, *81*, 3536.

(15) Grote, R. F.; Hynes, J. T. *J. Chem. Phys.* **1980**, *73*, 2715.

(16) Voth, G. A. *Chem. Phys. Lett.* **1990**, *170*, 289.

(17) Topper, R. Q.; Tawa, G. J.; Truhlar, D. G. *J. Chem. Phys.* **1992**, *97*, 3668.

(18) (a) Giachetti, R.; Tognetti, V. *Phys. Rev. Lett.* **1985**, *55*, 912. (b) Giachetti, R.; Tognetti, V. *Phys. Rev. B* **1985**, *33*, 7647.

(19) (a) Warshel, A.; Creighton, S. In *Computer Simulations of Biomolecular Systems*; van Gunsteren, W. F., Weiner, P. K., Eds.; ESCOM: Leiden, The Netherlands, 1989; pp 120–138. (b) Lee, F. S.; Chu, Z. T.; Warshel, A. *J. Comput. Chem.* **1993**, *14*, 161.

(20) King, G.; Warshel, A. *J. Chem. Phys.* **1989**, *91*, 3647.

(21) (a) Warshel, A. *Computer Modeling of Chemical Reactions*; John Wiley and Sons, Inc.: New York, 1991. (b) Hwang, J.-K.; King, G.; Creighton, S.; Warshel, A. *J. Am. Chem. Soc.* **1988**, *110*, 5297.

(22) It is important to recognize that the formal basis of eq 11 is different from the approximation presented by Feynman and Hibbs.[12a] The main difference is that eqs 8 and 11 are formally exact equations.